The microwave surface impedance of ultra-pure superconducting metals

2001 J. Phys.: Condens. Matter 13 L65

(http://iopscience.iop.org/0953-8984/13/4/101)

INSTITUTE OF PHYSICS PUBLISHING JOURNAL OF PHYSICS: CONDENSED MATTER

J. Phys.: Condens. Matter **13** (2001) L65–L71 www.iop.org/Journals/cm PII: S0953-8984(01)17984-1

LETTER TO THE EDITOR

The microwave surface impedance of ultra-pure superconducting metals

M A Hein[1], **R J Ormeno and C E Gough**

School of Physics and Astronomy, The University of Birmingham, Edgbaston, Birmingham B15 2TT, UK

Received 13 October 2000, in final form 27 November 2000

Abstract

Quasiparticle relaxation and non-local effects on the surface impedance Z_s of pure metals are analysed for arbitrary relaxation times τ and mean free paths l. The analysis predicts a non-monotonic variation of the differential loss tangent $(\partial R_s/\partial\tau)/(\partial X_s/\partial\tau)$ in the *normal state*, which distinguishes it from the classical limits. In the *superconducting* state, Z_s can be described by a two-fluid model incorporating a Drude-type conductivity and an effective relaxation time τ_e. The τ-values derived from theory and data measured on Sr_2RuO_4-crystals using a hollow dielectric resonator technique at 10 GHz are consistent, and in accordance with DC resistivity data.

Studying the electrodynamic response of the metallic copper-free layered perovskite Sr_2RuO_4 [1,2] at microwave frequencies $\omega = 2\pi f$, provides information on the electronic properties within a surface layer of the order of the reduced plasma wavelength ∼200 nm, and on a time scale of the order of $1/\omega$. Such measurements are therefore complementary to thermodynamic measurements of bulk properties and low-frequency transport measurements, which are insensitive to quasiparticle scattering. Investigating the surface impedance Z_s of Sr_2RuO_4 is of special interest because of its very high purity [2], which enhances relaxation and non-local effects at microwave frequencies. There is also increasing evidence that the superconducting order parameter of this spin-triplet superconductor has a p-wave symmetry [3–5].

In the *normal state* of Sr_2RuO_4, the long quasiparticle relaxation time τ renders the microwave response intermediate between the local and non-local limits leading to the normal and extreme anomalous skin effects [6]. The limiting regimes are determined by the ratios of the classical skin depth $\delta = (2\rho/\mu_0\omega)^{1/2}$ to either the quasiparticle mean free path $l = v_F\tau$ or the path $L_\omega = v_F\tau_\omega$ travelled in the time $\tau_\omega = 1/\omega$ (v_F is the Fermi velocity, μ_0 the vacuum permeability, and ρ the DC resistivity, with typical values for high-purity crystals of around 0.2 $\mu\Omega$ cm at T_c [7]). At a typical microwave frequency $f = 10$ GHz, $\delta \approx 225$ nm is only about one third of the in-plane mean free path $l \sim 700$ nm of high-purity Sr_2RuO_4 [7]. While the low-frequency condition for the normal skin effect limit, $l \ll \delta(\omega)$ [6], is violated, a local electrodynamic response might be restored at high frequencies if $L_\omega \ll \delta/(\omega\tau)^{1/2}$ [6]. However, with $v_F \sim 8\times10^4$ m s^{-1} typical for Sr_2RuO_4 [8], we obtain $L_\omega \approx 1200$ nm and

[1] On leave from Department of Physics, University of Wuppertal, Germany

$\delta/(\omega\tau)^{1/2} \approx 400$ nm at 10 GHz. Hence, neither the normal nor the extreme anomalous skin effects are appropriate to describe the surface impedance of Sr_2RuO_4 in the normal state.

Recent microwave measurements in the *superconducting* state of high-purity Sr_2RuO_4 crystals have revealed an unusual non-monotonic temperature dependence of the effective microwave penetration depth below T_c (see figure 4(a), inset to figure 5 and [9]). This effect results from the similarity in magnitude of δ and the reduced plasma wavelength $\Delta_p = \lambda_p/2\pi = (m^*/\mu_0 n_0 e^2)^{1/2} \sim 150$ nm, which causes comparably large contributions to the shielding of microwave fields by quasiparticles and Cooper pairs near T_c (n_0 is the effective quasiparticle density and m^* their effective mass). The Z_s-data can be described by a two-fluid model with a Drude-like quasiparticle conductivity and an effective relaxation time $\tau_e \sim 1/\omega$, allowing us to derive an extrapolated finite fraction of unpaired charge carriers at zero temperature and a quadratic temperature dependence of λ_L [9]. The basic features of this model are sketched in the second part of this paper.

To model the *normal state* surface impedance of Sr_2RuO_4 properly, we have extended the theory of Reuter and Sondheimer (RS) [6] to arbitrary values of the dimensionless scattering time $\omega\tau$ and non-locality parameter $\beta \equiv 0.75(L_\omega/\Delta_p)^2$; Δ_p represents the shortest length scale for the penetration of magnetic fields into a clean metal. The RS analysis assumes an isotropic Fermi surface and scattering time, a quadratic quasiparticle dispersion relation, and specular or completely diffuse reflection at the surface (see also [10]). For simplicity, we focus on specular reflection, which reveals the essential features of the problem. The assumption of an isotropic Fermi surface does not apply to Sr_2RuO_4, where it consists of three almost cylindrical sheets [11]. However, for our measurements with the microwave magnetic field parallel to the c-axis of the crystal and the induced currents both flowing and decaying parallel to the RuO_2 planes, the difference between a cylindrical and a spherical Fermi surface introduces only minor corrections.

To calculate the surface impedance Z_s, RS derived a general relation between current density and electric field for arbitrary values of l [6]. We combine their equations (21), (40) and (41) and express Z_s entirely in terms of $\omega\tau$, by replacing l by $v_F\tau$:

$$Z_s = R_s + \mathrm{i}X_s = \frac{2\mathrm{i}}{\pi}\mu_0 v_F \frac{\omega\tau}{1+\mathrm{i}\omega\tau} \int_0^\infty \frac{\mathrm{d}q'}{q'^2 + \mathrm{i}\beta\kappa(q')\,[\omega\tau/(1+\mathrm{i}\omega\tau)]^3}. \qquad (1)$$

The electromagnetic response is local if the material-specific frequency dependent parameter β is much smaller than $\beta_c \equiv [1 + 1/(\omega\tau)^2]^{3/2}$ [6,12], as illustrated in figure 1(a). This generalises the limits $l \ll \delta$ and $\mathrm{x}_\omega \ll \delta/(\omega\tau)^{1/2}$ at low and high frequencies.

The function $\kappa(q') = 2[(1 + q'^2)\tan^{-1}(q') - q']/q'^3$ in equation (1) is plotted in figure 1(b). It is related to the wave-number dependent transverse conductivity [13,14] by $\sigma(q)/\sigma_0 = 0.75\kappa(q')/(1 + \mathrm{i}\omega\tau)$, where $q' = ql/(1 + \mathrm{i}\omega\tau)$ and σ_0 is the DC conductivity. Relaxation and non-local effects on Z_s are related to the functional dependence of κ on q' [15]. The normal limit is obtained by replacing $\kappa(q')$ by its asymptotic value $\kappa_0 = 4/3$ as $q' \to 0$, yielding:

$$\frac{Z_{s,0}}{\mu_0\omega\Delta_p} = \left[1 + \frac{1}{(\omega\tau)^2}\right]^{1/4} \left\{\sin\left[\frac{\tan^{-1}(1/\omega\tau)}{2}\right] + \mathrm{i}\cos\left[\frac{\tan^{-1}(1/\omega\tau)}{2}\right]\right\}. \qquad (2)$$

Equation (2) is the local-limit result $Z_{s,0} = (1 + \mathrm{i}\omega\tau)^{1/2}(\mathrm{i}\omega\mu_0/\sigma_0)^{1/2}$ for a Drude-type quasiparticle conductivity $\sigma_0/(1 + \mathrm{i}\omega\tau)$ [9], which reduces to the classical skin effect result $Z_{s,\mathrm{class}} = \mu_0\omega\Delta(2/\omega\tau)^{1/2}(1 + \mathrm{i})$ for $\omega\tau \ll 1$. Similarly, the extreme anomalous limit is obtained from equation (1) by replacing $\kappa(q')$ by its asymptotic value $\kappa_\infty(q') = \pi/q'$ as $q' \to \infty$. The resulting surface impedance is $Z_{s,\infty} = \gamma\mu_0\omega\Delta_p\beta^{1/6}(1 + \mathrm{i}\sqrt{3})$ with $\gamma^{-1} = 9(8\pi)^{1/3}/8$.

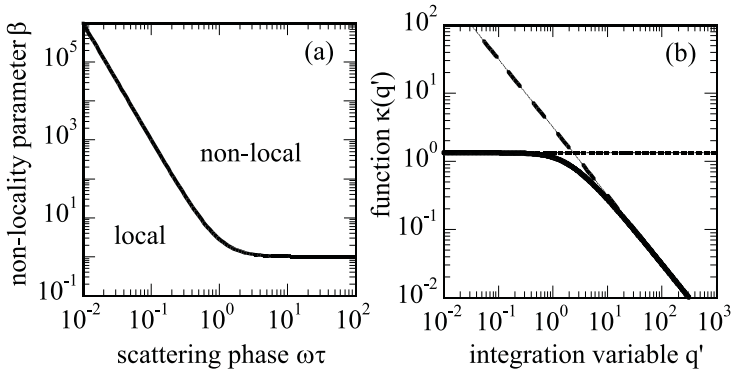

Figure 1. (a) Critical non-locality parameter β versus $\omega\tau$, separating local and non-local response as indicated. (b) Illustration of $\kappa(q')$ (solid curve) and its asymptotic behaviour 4/3 (dotted) and π/q' (dashed line).

The results for the local and extreme anomalous limits are displayed in figure 2 as the normalized surface resistance $R_s/R_{s,\infty}$ (curves 1a and 2a) and surface reactance $X_s/R_{s,\infty}$ (1b and 2b) versus $\omega\tau$. We note that $R_{s,0}$ decreases below $R_{s,\infty}$ like $1/\omega\tau$ in the limit of large $\omega\tau$, while $X_{s,0}/R_{s,\infty}$ approaches a β-dependent value independent of $\omega\tau$. According to equation (2), the ratio $R_{s,0}/X_{s,0}$ is given by $\tan[\tan^{-1}(1/\omega\tau)/2] = [1 + (\omega\tau)^2]^{1/2} - \omega\tau$.

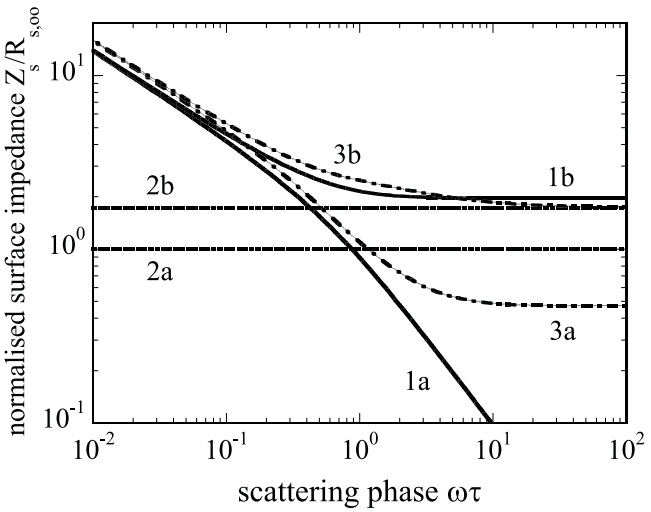

Figure 2. $\omega\tau$-dependence of $R_s/R_{s,\infty}$ and $X_s/R_{s,\infty}$ for the normal limit (curves 1a and 1b) and the extreme anomalous limit (2a and 2b). The analytical approximation to equation (1) described in the text is illustrated for the intermediate case $\beta = 10$ (3a and 3b). All curves were evaluated for $v_F = 8\times10^4$ m s^{-1} and $f = 10$ GHz.

RS discussed the analytical solution of equation (1) only for the above approximations of κ for the two limits which, however, are justified only for small ($q' < 0.1$) and large ($q' \geqslant 30$) arguments (figure 1(b)). We obtain a more accurate analytical approximation of $Z_s(\omega\tau)$ by separating the integral (equation (1)) into two sections defined by the limiting forms of $\kappa(q')$

at low and high q'-values intersecting at $q' = 3\pi/4$. A typical result is illustrated in figure 2 for $\beta = 10$ (curves 3a and 3b). The deviation from the local limit at small $\omega\tau$-values is an artefact of the chosen normalization (see figure 3 below). Significant non-local corrections to the $\omega\tau$-dependence expected from equation (2) occur for this β-value at moderate values $\omega\tau \sim 0.5$. While X_s approaches the extreme anomalous limit at large $\omega\tau$, R_s approaches a β-dependent level well below $R_{s,\infty}$. R_s and X_s approach the extreme anomalous limit ratio $X_s/R_s = \sqrt{3}$ over an increasing range of $\omega\tau$-values for large values of β.

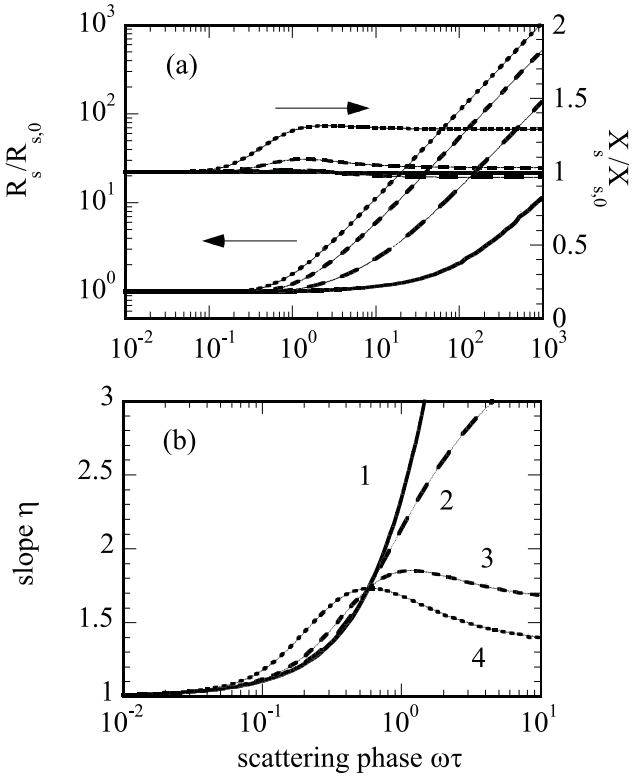

Figure 3. (a) $\omega\tau$-dependence of $R_s/R_{s,0}$ (left ordinate) and $X_s/R_{s,0}$ (right ordinate), resulting from the numerical solution of equation (1) for $\beta = 0.1$ (solid curve), 1 (coarse-dashed), 10 (fine-dashed), and 100 (dotted). (b) Differential loss tangent $\eta(\omega\tau) = (\partial R_s/\partial\tau)/(\partial X_s/\partial\tau)$ for $\beta = 0.1$, 1, 10, and 100 (1–4). All curves in both panels were evaluated for $v_F = 8\times10^4$ m s^{-1} and $f = 10$ GHz.

The above analytical but still approximate solution reveals the qualitative features of Z_s in the intermediate range of $\omega\tau$ and β-values. An exact solution of equation (1) requires numerical integration involving no approximations to $\kappa(q')$ [10]. Figure 3(a) shows computed R_s and X_s values, normalized to the values $R_{s,0}$ and $X_{s,0}$ in the pure relaxation limit (equation (2)), for $\beta = 0.1$ (solid), 1.0 (coarse dashed), 10 (fine dashed), and 100 (dotted). Non-local corrections to Z_s become important for $\omega\tau$-values which decrease with increasing β, as shown in figure 1(a).

The influence of non-locality on Z_s is illustrated further by the differential loss tangent $\eta \equiv (\partial R_s/\partial\tau)/(\partial X_s/\partial\tau)$ in figure 3(b). This quantity, which can be directly derived from measured data without absolute calibration, can be used to determine $\omega\tau$ for a given β-value.

In the local limit, the slope $\eta_0 = \{[1 + (\omega\tau)^2]^{1/2} - \omega\tau\}^{-1}$ increases continuously, consistent with equation (2). In contrast, our numerical results for $\beta = 0.1$, 1, 10, and 100 (curves 1 to 4) show a peak developing in η for $\omega\tau$-values which decrease with increasing β (around $\omega\tau \sim 0.1$–1 for $\beta = 10$–100, appropriate for Sr_2RuO_4 at 10 GHz). The position and the exact shape of the peak depend on the band structure of the metal through the parameters λ_p and v_F. The maximum of the differential loss tangent provides therefore a sensitive method to correlate microwave measurements of the normal state in high-purity metals with their Fermi surface properties.

Our theoretical results can be compared with experimental data on $Z_s(T)$ of high-purity Sr_2RuO_4 crystals measured at 10 GHz using a hollow dielectric resonator technique [16]. Normal state measurements were extended to temperatures $T \sim 0.4$ K by application of a DC magnetic field perpendicular to the RuO_2 planes. Figure 4(a) displays the essential results for the resonator bandwidth, $\Delta f_{B,\mathrm{tot}}(T)$, associated with the microwave losses (left ordinate) and for the change of the resonant frequency, $-2\Delta f_0(T)$, associated with the change of the penetration depth in the Sr_2RuO_4 crystal (right ordinate) with and without magnetic field (filled and open symbols). More details of our experimental results are being published separately [9]. Figure 4(b) shows the slope $\eta(T) = -[\partial(\Delta f_{B,\mathrm{tot}})/\partial T]/[\partial(2\Delta f_0)/\partial T]$ directly derived from these data. Above about 8 K, $\eta(T)$ approaches unity as expected in the normal skin effect limit, i.e. $\omega\tau < 0.1$. However, with decreasing temperature the slope increases but tends to saturate below 1 K, reflecting the increase of $\tau(T)$ towards a constant value limited by elastic impurity scattering. The derived value $\eta \sim 1.7$ is close to the maximum expected for Sr_2RuO_4 at 10 GHz ($\beta \sim$10–100) and occurs when $\omega\tau \sim$0.5–1, confirming that we are in neither the normal nor extreme anomalous skin effect limits.

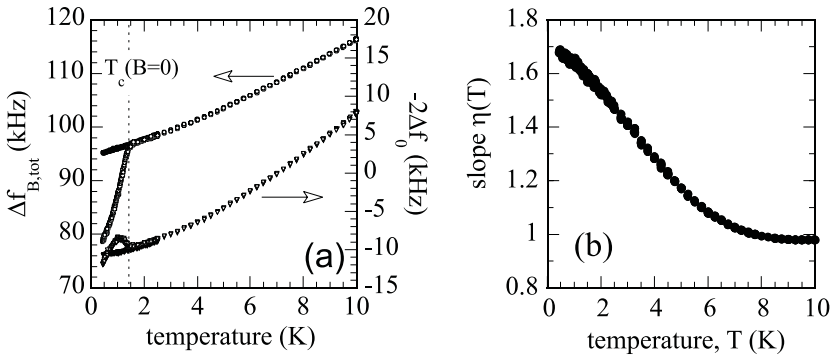

Figure 4. (a) Temperature dependence of the microwave impedance of a Sr_2RuO_4 crystal at 10 GHz (left ordinate: microwave losses, right ordinate: change of resonant frequency) in static magnetic field $B = 0$ mT (open) and $B = 63$ mT (filled symbols) [9]. (b) Differential loss tangent $\eta(T) = (\partial R_s/\partial T)/(\partial X_s/\partial T)$ deduced from the experimental data in panel (a).

Relaxation and non-locality have also to be considered in the *superconducting* state. However, since Sr_2RuO_4 is a type-II superconductor [8], the electrodynamic response of the Cooper pairs is essentially local. The non-locality and relaxation of the quasiparticle response can be approximated by a Drude-type quasiparticle conductivity replacing τ by an *effective* relaxation time τ_e. Expansion of $\kappa(q') \sim 4/3 \times (1 - q'^2/5)$ in equation (1) and comparison with equation (2) reveals that $\tau_e/\tau = 1 + 4/15 \times (l/\Delta_p)^2$ for $\beta < \beta_c$. (The two-fluid model with a local pair response and a non-local quasiparticle response will be analysed in greater detail in a separate paper.) Our assumptions lead to $Z_s = (\mathrm{i}\mu_0\omega/\sigma)^{1/2}$; the complex conductivity σ

is determined by the fractions $x_N(T)$ and $x_S(T) = 1-x_N(T)$ of unpaired and paired charge carriers, $\mu_0\omega\Delta_p^2\sigma = x_N\varphi_e/(1+\mathrm{i}\varphi_e)-\mathrm{i}x_S$, where $\varphi_e \equiv \omega\tau_e$. The result for Z_s, normalised to $R_s(x_N = 1)$, is

$$\frac{Z_s}{R_n} = x_N^{-1/2}\left[\frac{1+\varphi_e^2}{1+\epsilon^2}\right]^{1/4}\frac{\sin[\tan^{-1}(\epsilon^{-1})/2]+\mathrm{i}\cos[\tan^{-1}(\epsilon^{-1})/2]}{\sin[\tan^{-1}(\varphi_e^{-1})/2]} \tag{3}$$

with $\epsilon = \varphi_e + x_S/x_N\times(\varphi_e+\varphi_e^{-1})$. The modelled surface reactance X_s indeed passes through a maximum at $x_N < 1$, i.e. $T < T_c$, in accordance with our experimental data in figure 4(a). The maximum of X_s/R_n occurs at a value $\epsilon = \epsilon_0(\varphi_e)$ given by the positive root of the equation $(\epsilon_0+\varphi_e{}^{-1})^2-(1+\epsilon_0^2)^{1/2}(\epsilon_0+\varphi_e^{-1})-\varphi_e^{-2} = 1$. We note that the total increase of the reactance above its normal state value, $\xi_{\max} = [X_{s,\max} - X_s(1)]/R_n$, depends only on φ_e:

$$\xi_{\max} = \frac{1}{\tan[\tan^{-1}(\epsilon_0^{-1})/2]}\times\left[\frac{(1+\epsilon_0\varphi_e)^2}{(1+\varphi_e^2)(1+\epsilon_0^2)}\right]^{1/4} - \frac{1}{\tan[\tan^{-1}(\varphi_e^{-1})/2]}. \tag{4}$$

Equation (4) is plotted in the main body of figure 5. Our model can be easily compared with the experimental data if we plot the surface reactance (figure 4(a)) against the surface resistance, both normalized to $R_s(T_c)$ (see inset to figure 5). The implicit variable in this parametric plot is, in the experiment, the temperature T, while it is x_N in the two-fluid model. The parameter $\xi_{\max}$ can be obtained from a comparison between data and model without knowing absolute values of Z_s as indicated, therefore allowing an unambiguous determination of φ_e. The inset to figure 5 shows that the surface impedance of Sr_2RuO_4 measured at 10 GHz can be described very well throughout the superconducting state with a constant value $\varphi_e = 0.78$. This value is consistent with $\omega\tau \sim 0.5$ derived from the normal state microwave measurements and a typical DC resistivity $\rho(T_c) = \mu_0\Delta_p^2\tau \sim 0.2\,\mu\Omega$ cm [7].

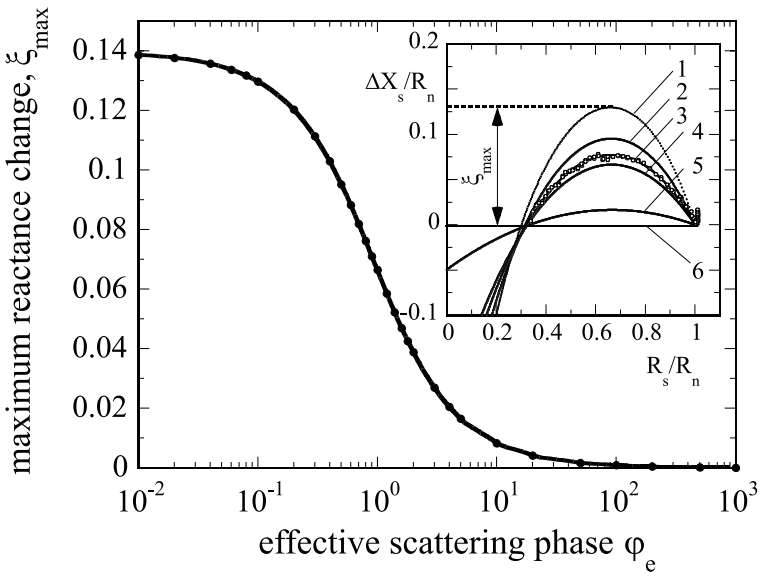

Figure 5. φ_e-dependence of $\xi_{\max}$ (dots: evaluation of equation (4) at selected values of φ_e, solid curve: interpolation). Inset: parametric plot of Z_s/R_n, with $\Delta X_s(x_N) = X_s(x_N)-X_s(1)$, according to equation (3) for $\varphi_e = 0.1, 0.5, 0.78, 1.0, 5.0, \infty$ (1–6). The definition of $\xi_{\max}$ is indicated for curve 1. The symbols represent data on a Sr_2RuO_4 crystal at 10 GHz [9].

Once the effective scattering time τ_e is known, equation (3) can be used to derive the normal fraction $x_N(T)$ from the measured $Z_s(T)$ data. As discussed in more detail in [9], we find $x_N(T)$ extrapolating almost linearly to a finite value at zero temperature.

In summary, we have studied the effect of quasiparticle relaxation and non-locality on the surface impedance of the high-purity superconducting metal Sr_2RuO_4. We have analysed the Reuter and Sondheimer theory for arbitrary values of $\omega\tau$ and non-locality parameter $\beta \sim (l/\lambda_p \times 1/\omega\tau)^2$. We compare the solutions for Z_s with the local description and find good agreement up to β-values close to the critical value $\beta_c(\omega\tau)$. We predict a peak in the differential loss tangent $\partial R_s/\partial X_s$, which provides a sensitive method to correlate normal-state microwave measurements of high-purity metals with their Fermi surface properties. In the superconducting state, Z_s can be described by a local two-fluid model, which enables us to determine an effective scattering time τ_e below T_c. We find a temperature independent τ_e-value throughout the superconducting state. The derived τ-values in the normal and superconducting states are consistent and in good agreement with DC resistivity data.

We are grateful to A P Mackenzie, G Müller, K Scharnberg, R Schwab and A Sibley for valuable discussions and to Y Maeno for providing us with the high-purity Sr_2RuO_4 crystals. MAH thanks the EPSRC (UK) and the Land Nordrhein-Westfalen (Germany) for financial support.

References

[1] Randall J J and Ward R J 1959 *Am. Chem. Soc.* **81** 2629
[2] Maeno Y, Hashimoto H, Yoshida K, Nishizaki S, Fujita T , Bednorz J G and Lichtenberg F 1994 *Nature* **372** 532
[3] Mackenzie A P and Maeno Y 2000 *J. Low Temp. Phys.* **117**
[4] Rice T M and Sigrist M 1995 *J. Phys.: Condens. Matter* **7** L643
[5] Baskaran G 1996 *Physica* B **223–224** 490
[6] Reuter G E H and Sondheimer E H 1948 *Proc. R. Soc.* **195** 336
[7] Mackenzie A P *et al* 1998 *Phys. Rev. Lett.* **80** 161 erratum, ibid. 3890
[8] Riseman T M *et al* 1998 *Nature* **396** 242
[9] Ormeno J, Hein M A, Sibley A, Gough C E, Mao Z Q and Maeno Y 2000 *The surface impedance and penetration depth of Sr_2RuO_4* preprint
[10] Zuccaro C 1995 Doctoral Thesis University of Hamburg; unpublished
[11] Mackenzie A P *et al* 1996 *Phys. Rev. Lett.* **76** 3786
[12] Chambers R G 1952 *Proc. R. Soc.* A **215** 481
[13] Pippard A B 1960 *Rep. Progr. Phys.* **23** 176
[14] Kittel C 1963 *Quantum Theory of Solids* (New York: Wiley)
[15] Scharnberg K 1978 *J. Low Temp. Phys.* **30** 229
[16] Wingfield J J *et al* 1997 *IEEE Trans. Appl. Supercond.* **7** 2009